arXiv:1302.6596v1 [cond-mat.str-el] 26 Feb 2013

Quantum Simulation Architecture for Lattice Bosons in Arbitrary, Tunable External Gauge Fields

Eliot Kapit
Rudolf Peierls Center for Theoretical Physics, Oxford University,
1 Keble Road, Oxford OX1 3NP, United Kingdom[*]

We describe a lattice of asymmetrical qubit pairs in one or two dimensions, with couplings arranged so that the motion of single-qubit excited states mimics the behavior of charged lattice bosons hopping in a magnetic field. We show in particular that one can tune the parameters of the many-body circuit to reach a regime where the complex hopping phase between any two elements can be tuned by simply adjusting the relative phases of two applied oscillating voltage signals. We also propose a specific realization of our model using coupled three junction flux qubits, in which one can reach the strongly interacting bosonic quantum Hall limit where one will find anyonic excitations. The circuits could be used for topological quantum computation.

PACS numbers: 73.43-f,03.67.-a,75.10.Kt

I. INTRODUCTION

Fractional quantum Hall effects [1–3] are among the most profound collections of phenomena to emerge in interacting quantum many-body systems. The elementary excitations in these systems do not act like bosons or fermions; rather, they are *anyons*, which in some cases can be used for a robust form of quantum computing [4, 5]. All physical examples of fractional quantum Hall effects are in two dimensional (2D) electron gases. Here we propose a method for linking standard qubit designs which will realize a *bosonic* fractional quantum Hall effect. The rich theoretical literature on bosonic fractional quantum Hall effects suggests that there will be a large number of interesting states [6–13] that could be explored in our system. These include 'Pfaffians' and their generalizations. Furthermore, one could anticipate that some important experiments (such as directly braiding quasiparticles) may be simpler in a qubit array than in a GaAs layer surrounded by AlGaAs.

There are several competing approaches to engineering bosonic fractional quantum Hall effects. One proposal uses Raman lasers to simulate the magnetic vector potential in neutral cold atoms [14, 15]. The technical challenges are, however, quite daunting: new cooling methods need to be designed to offset heating from the Raman lasers, and the most natural probes are indirect. Another scheme is to use lattices of tiny superconducting grains (charge qubits, [16–21]) connected through Josephson junctions. Suitably low temperatures can be reached in a dilution refrigerator, and the system is readily studied using transport measurements. Unfortunately, random charge noise, which scales linearly with the interaction strength, would prevent the quantum Hall regime from being reached without significant local tuning of the potentials on hundreds or thousands of lattice sites. Other proposals include superconducting Jaynes-Cummings lattices [22] and "photon lattices" of coupled optical waveguides [23–25], each of which have their own advantages and shortcomings.

We here propose a new and promising approach. Namely, we consider a circuit of qubits, with a geometry which naturally maps onto a system of charged bosons hopping in a magnetic field. In order to produce complex hopping matrix elements we propose a lattice of coupled asymmetrical pairs of qubits, which we label as A or B. We choose device parameters so that excitation energy ω_A of the A qubits is significantly smaller than the excitation energy of the B qubits, and place a B qubit on each link between neighboring A qubits. Further, we couple them to each other through alternating hopping ($\sigma_A^+ \sigma_B^- + H.C.$, henceforth referred to as a "±" coupling) and potential ($\sigma_A^z \sigma_B^z$, a "zz" coupling) terms. We also apply an external oscillating electromagnetic field of frequency ω to each qubit, with the relative phase of the signal applied to the B qubits shifted relative to that of the A qubits by a locally tunable φ_s. Since the B qubits are higher energy than the A qubits, we can integrate them out, leading to complex tunneling matrix elements (the amplitude of a process where the states of neighboring qubit pairs are exchanged) between A qubits with phases that can be tuned to any value by adjusting φ_s.

As we will describe below, a particularly attractive realization of this architecture would be to use three junction "flux qubits" (FQs) [26–35]. The flux qubits are mesoscopic superconducting rings interrupted by three Josephson junctions, placed in a magnetic field which is tuned so that nearly 1/2 of a magnetic flux quantum penetrates the ring. The energies of the flux qubits can be tuned by adjusting this magnetic field, or by varying the areas of the Josephson junctions, so that the B qubits are higher energy than the A qubits as outlined above. We then capacitively couple all the flux qubits to an external, oscillating voltage $V_0 \sin \omega t$, and arrange the couplings so that the phases of the voltage applied to the B qubits are shifted relative to the A qubits. The subtle interplay

---

[*] Electronic address: eliot.kapit@physics.ox.ac.uk

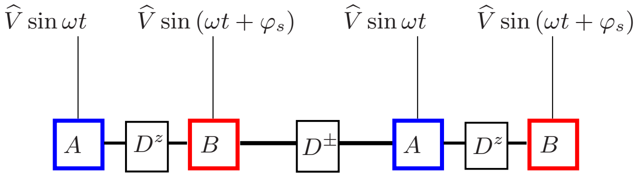
$\widehat{V}\sin\omega t$
$\widehat{V}\sin(\omega t+\varphi_s)$
$\widehat{V}\sin\omega t$
$\widehat{V}\sin(\omega t+\varphi_s)$
A
D^z
B
$D^\pm$
A
D^z
B

FIG. 1: Basic coupling structure for the A and B qubits. Each site in our many-body lattice would correspond to a single A qubit, which couples to its neighbors through one B qubit per link, joined through alternating hopping ($\pm$) and potential (zz) couplings as described in section II. Though drawn in one dimension in the figure, we ultimately intend to construct 2d lattices in this manner, and generalizations to even higher dimensions are also possible.

of the oscillating applied voltages with the mix of charge (capacitive) and phase (Josephson) couplings introduces phase shifts which make these hopping matrix elements complex, mimicking the Peierls phases found for charged particles in magnetic fields.

All of our flux qubits are operated in the regime where the Josephson energy $E_{\rm J}$ is large compared to the charging energy $E_{\rm C}$, so charge noise effects are exponentially suppressed. The system is therefore almost completely insensitive to stray low-frequency electric fields. The many-body excitation gap, a key feature of anyon states, can be measured through the single-qubit response to applied oscillating voltages. The large nonlinearities of the flux qubit devices imply that the first excited states experience an effectively infinite on-site repulsion. We note also that our scheme is not intended to function as a circuit QED architecture (in contrast to the recent work of Koch *et al* [36, 37] and others); the device parameters should be chosen so that the external voltages can be treated as purely classical sources, with no dynamical photons present in our system.

The remainder of this paper is organized as follows. In section II, we write down the basic coupled qubit Hamiltonian, and outline the conditions under which arbitrary external gauge fields can be simulated. In section III, we describe three junction flux qubits, and how they can be coupled to obtain the arbitrary complex hopping phases derived in section II. Having derived these phases, in section IV we show how the circuits of the two previous sections can be used as building blocks for exotic boson fractional quantum Hall states. Finally, in section V, we show how a simple arrangement of four flux qubits could experimentally demonstrate a nonzero effective gauge field, and offer concluding remarks.

II. GENERAL FORMALISM

A. Berry's Phase of a Rotating Spin

Before outlining the physics of our qubit array, we would first like to discuss a simple example to more straightforwardly elucidate the origin of the complex hopping phases. Specifically, we will consider a pair of spins and examine the Berry's phase effects generated during a process where an excitation is transfered from one spin to its neighbor (whose eigenstates lie on a different axis from the first spin) by rotating both spins about z and then transferred back by rotating both spins about y. Specifically, let us consider two initially uncoupled spin-$\frac{1}{2}$ degrees of freedom, with the Hamiltonian,

$$H = \sigma_A^x + \cos\theta\sigma_B^z + \sin\theta\left(\cos\varphi\sigma_B^x + \sin\varphi\sigma_B^y\right). \qquad (1)$$

Let us assume that initially spin A is excited and spin B is in its ground state. We first act with the operator $\sigma_A^z\sigma_B^z$ to transfer the excitation from A to B, and assume energy is conserved in this process so that the final state after acting with $\sigma_A^z\sigma_B^z$ is $|0_A 1_B\rangle$. We then act with $\sigma_A^y\sigma_B^y$ to transfer the excitation back; the resulting matrix element $\mathcal{M}$ for the entire process is

$$\begin{aligned}\mathcal{M} &= \langle 1_A 0_B|\,\sigma_A^y\sigma_B^y\,|0_A 1_B\rangle\,\langle 0_A 1_B|\,\sigma_A^z\sigma_B^z\,|1_A 0_B\rangle \qquad (2)\\ &= \sin\theta\left(\cos\varphi + i\sin\varphi\cos\theta\right).\end{aligned}$$

For $\theta \neq \pi/2$ and $\varphi \neq 0,\pi$, $\mathcal{M}$ is complex, and the resulting phase can be understood as a consequence of the Berry's phase acquired by a rotating spin, though we note of course that the Berry's phase discussed here is only an analogy, since we are considering the action of pairs of operators and not continuous, adiabatic changes to the system's wavefunction. When a spin m is rotated along a closed path, the resulting phase is equal to m times the area subtended by the path on the unit sphere. In this case, we have two spins which rotate, but both end in the same states in which they started, so we obtain a gauge-invariant phase equal to the sum of the phases picked up by both spins. The area subtended by A is just π, but the area subtended by B depends on the projection of σ_y and σ_z onto its quantization axis, and thus depends on φ_s, yielding the result above. Note that if we'd acted with $\sigma_A^z\sigma_B^z$ or $\sigma_A^y\sigma_B^y$ twice instead of using a combination of the two, the outcome would necessarily be real, since $\mathcal{M}$ would be the product of a matrix element and its Hermitian conjugate. In the Berry's phase picture, the phase is zero simply because the path of each spin's rotation would be a 1d line, and thus each area is zero. Both inequivalent eigenstates and anisotropic operations are necessary for spin transfer matrix element to be complex.

It is precisely this effect–the phase picked up by a spin which rotates as it propagates in space–which we will use to engineer artificial hopping phases in our lattice. Specifically, imagine the case in which we had two (identical) A spins with a B spin in between them, and after acting with $\sigma^z_{A1}\sigma^z_B$ to pass an excitation from $A1$ to the B spin, we then act with $\sigma^y_{A2}\sigma^y_B$ to transfer the excitation to the second A qubit instead of sending it back to the first. Since the A spins are identical, the matrix element $\mathcal{M}$ should be the same as the one derived above, and therefore by letting B spins mediate a hopping coupling, we can introduce tunable phases in a lattice of A spins.

Engineering this structure in a real spin (or qubit) lattice is by no means trivial. For real spins, one could introduce a spatially varying magnetic field to generate the inequivalent local eigenstates, but adding the anisotropic spin-spin interactions ($\sigma^z_A\sigma^z_B$ or $\sigma^y_A\sigma^y_B$ instead of $\mathbf{S}_A\cdot\mathbf{S}_B$) is very difficult. Conversely, for a more general lattice of qubits, generating passive anisotropic couplings is often straightforward, but generating inequivalent local eigenstates is not. We here demonstrate that coupling the qubits to a continuously oscillating monochromatic external field can introduce the required rotations, provided that the phases of the signals applied to the B qubits are different from those applied to the A qubits. By adjusting these phases at a local level, we can independently tune the tunneling phase between any linked sites on the lattice, and can thus simulate any desired external gauge field, at least in principle.

B. Qubit Coupling Hamiltonian

We will consider a lattice of qubits, arranged such that there is an asymmetric pair of qubits A and B at each site. We shall assume throughout that the following conditions hold:

(1) The nonlinearities of each physical system which we use as a qubit are large enough that we can consider them to be purely two-level systems, and ignore all eigenstates besides $|0\rangle$ and $|1\rangle$. This requirement ultimately constrains the magnitudes of the couplings between qubits, which must be small compared to the physical devices' absolute nonlinearities.

(2) The qubits can be coupled to an external electromagnetic field. We shall further require that the electromagnetic field operator $\widehat{V}$ (which could represent the coupling to magnetic fields as well) has no expectation value in either state, so $\langle 0|\widehat{V}|0\rangle = \langle 1|\widehat{V}|1\rangle = 0$. These fields will always be present in the qubit array Hamiltonian, and we will treat them in the standard rotating wave approximation.

(3) We must be able to introduce two types of coupling between the qubits, so that the qubit-qubit Hamiltonian takes the form

$$H_{int} = D^{\pm}\left(\sigma^+_A\sigma^-_B + \sigma^-_A\sigma^+_B\right) + D^z\sigma^z_A\sigma^z_B. \tag{3}$$

We must have independent control over both $D^{\pm}$ and D^z for our method to succeed. Note that any physical coupling between the qubits will typically include terms which violate number conservation. However, when we transform to the rotating frame when the external oscillating voltage is applied, the terms in H_{int} are unchanged but anomalous terms such as $\sigma^-_A\sigma^z_B$ or $\sigma^+_A\sigma^+_B$ will become rapidly oscillating and can be dropped from the low-energy Hamiltonian.

(4) We must be able to tune the relative phase φ_s of the external electromagnetic field applied to B qubits relative to the A qubits, as shown in fig. 1. If $\varphi_s \neq 0, \pi$ then time reversal symmetry is broken, since we cannot chose a zero point for the time t so that both $V_A(t) = V_A(-t)$ and $V_B(t) = V_B(-t)$. Breaking time reversal symmetry is a basic requirement for obtaining nontrivial effective gauge fields.

These requirements could be fulfilled by a large number of physical systems, including spin qubits, trapped ions, and superconducting devices, which will be the focus of this work. Let us now consider the Hamiltonian of a given qubit pair, H_{AB}. Before turning on the oscillating fields, our qubit Hamiltonian is

$$\begin{aligned} H^0_{AB} &= \omega_A\sigma^z_A + \omega_B\sigma^z_B \\ &\quad + \left\{D^{\pm}\left(\sigma^+_A\sigma^-_B + \sigma^-_A\sigma^+_B\right) \text{ or } D^z\sigma^z_A\sigma^z_B\right\}. \end{aligned} \tag{4}$$

We now turn on the oscillating fields. When acting on A or B, we have:

$$\widehat{V} = 2\Omega_{A/B}\sigma^y_{A/B}, \tag{5}$$

with $2\Omega_{A/B} = \left\langle 1_{A/B}\right|\widehat{V}\left|0_{A/B}\right\rangle$, which we choose to be real (in the flux qubits described below, the full matrix element for the $\widehat{V}$ operator is imaginary, but we have absorbed those factors of i into σ^y). We now examine

$$\begin{aligned} \widehat{V}\sin\omega t &= \Omega_{A/B}\left(e^{i\omega t}\sigma^-_{A/B} + e^{-i\omega t}\sigma^+_{A/B}\right) \\ &\quad + \Omega_{A/B}\left(e^{-i\omega t}\sigma^-_{A/B} + e^{i\omega t}\sigma^+_{A/B}\right). \end{aligned} \tag{6}$$

We now transform to the rotating frame by applying the unitary transformation $|\psi\rangle \rightarrow \exp -i\omega\left(\sigma^z_A + \sigma^z_B\right)t\,|\psi\rangle$. The time dependence of terms on the first line of (6) is cancelled out, leaving us with $\Omega_{A/B}\sigma^x_{A/B}$ plus a set of terms which are rapidly oscillating with frequency 2ω. We now make the rotating wave approximation (RWA) to neglect these terms; if further accuracy is required we can treat them through a second order perturbation theory in $\left(\Omega_{A/B}/\omega\right)$ and obtain a small correction to the $\sigma^z_{A/B}$ terms. After transforming to the rotating frame and invoking the RWA, H_{AB} is:

$$\begin{aligned} H_{AB} &= \left(\omega_A - \omega\right)\sigma^z_A + \left(\omega_B - \omega\right)\sigma^z_B \\ &\quad + \Omega_A\sigma^x_A + \Omega_B\left(\cos\varphi_s\sigma^x_B + \sin\varphi_s\sigma^y_B\right) \\ &\quad + \left\{D^{\pm}\left(\sigma^+_A\sigma^-_B + \sigma^-_A\sigma^+_B\right) \text{ or } D^z\sigma^z_A\sigma^z_B\right\}. \end{aligned} \tag{7}$$

From now on we will assume ω is tuned to resonance with the A qubits, so that $\omega = \omega_A$ and the single-site Hamiltonian for the A qubits is just $\Omega_A\sigma^x_A$.

To construct the full qubit lattice, we wire the qubits as in fig. 1, so that the connection between any pair of neighboring A qubits consists of a zz coupling to a B qubit followed by a $\pm$ coupling to the neighboring A qubit. For simplicity, we will ignore cases where A qubits are coupled directly; such couplings will produce either neighbor-neighbor potential interactions or real-valued hopping matrix elements, depending on their structure. We assume that the energy difference $E_B - E_A = 2\sqrt{(\omega_B-\omega_A)^2+\Omega_B^2} - 2\Omega_A \equiv \delta E$ is large compared to $D^{\pm}$ and D^z, so that we can treat the $A-B$ coupling perturbatively. We now eliminate the B qubits using second order perturbation theory; noting that all A qubits are identical, the resulting Hamiltonian, to order $D^2/\delta E$, is given by:

$$\begin{aligned} H &= \sum_{ij}\left(J_{ij}a_i^{\dagger}a_j + H.C.\right) + 2\tilde{\Omega}_A\sum_i a_i^{\dagger}a_i, \qquad (8)\\ J_{ij} &= -\frac{D_{ij}^z D_{ij}^{\pm}}{\delta E}\sin\theta\left(\cos\varphi_{s(ij)} + i\cos\theta\sin\varphi_{s(ij)}\right),\\ \cos\theta &= \frac{\omega_B-\omega_A}{\sqrt{(\omega_B-\omega_A)^2+\Omega_B^2}}. \end{aligned}$$

Here $a_i^{\dagger}/a_i$ creates/annihilates an excitation in the A qubit at site i, and $\tilde{\Omega}_A$ is equal to Ω_A plus $O(J)$ shifts which depend on the coordination number of the lattice and magnitudes of the couplings. Since the qubits are spin-$\frac{1}{2}$, we have an effective hard-core constraint, so $a_i^{\dagger}|1_i\rangle = 0$. If we now identify

$$\arg J_{ij} \equiv q\int_{r_i}^{r_j}\mathbf{A}\cdot d\mathbf{r}, \qquad (9)$$

we see that the complex phases of J are identical to the Peierls phases of a charged particle moving on a lattice in an external gauge field $\mathbf{A}$. Further, if we choose parameters so that the B qubits are far off-resonance, θ will be small and

$$J_{ij} \to -\frac{D_{ij}^z D_{ij}^{\pm}}{\delta E}\theta e^{i\varphi_{s(ij)}} + O\left(\theta^3\right). \qquad (10)$$

In this regime, we can freely adjust the phase of J without significantly altering its magnitude, and can thus simulate any time-dependent external gauge field configuration we desire, simply by adjusting the B qubit phase shifts $\varphi_{s(ij)}$ at each link.

The ability to engineer artificial gauge fields of any desired configuration has tremendous potential to unlock new physics, and we will discuss the most natural application, simulating a uniform magnetic field to realize strongly interacting bosons in the quantum Hall regime, later in the work. Before doing so, however, we will first describe a possible implementation of this architecture in superconducting flux qubits. While flux qubits are certainly not the only– or even necessarily the best– qubits to use for this purpose, our proposal will demonstrate that a fairly robust implementation of our architecture can be realized using device parameters from previous experiments. Thus, small lattices should be within reach of current technology.

III. FLUX QUBITS

The three-junction flux qubit consists of a superconducting ring interrupted by three Josephson junctions as shown in fig. 2, with one junction whose area is rescaled by α relative to the other two. A constant, tunable magnetic flux bias of $f \neq 1/2$ flux quanta is applied through the loop. We choose bottom third of the ring to be ground (which will be a physical ground in our case) with phase $\phi = 0$, then the two remaining degrees of freedom of the flux qubit are the phases ϕ_1 and ϕ_2 of the other two superconducting regions. The derivation of the flux qubit Hamiltonian is descrbed in detail in Orlando *et al* [27]; in terms of the phases ϕ_1 and ϕ_2, the flux qubit Hamiltonian H_{FQ} is

$$\begin{aligned} H_{FQ} &= \frac{(1+\alpha+\eta)\left(Q_1^2+Q_2^2\right)+2\alpha Q_1Q_2}{(1+\eta)(1+2\alpha+\eta)C} \qquad (11)\\ &\quad -E_{\mathrm{J}}\left[\cos\phi_1+\cos\phi_2+\alpha\cos\left(2\pi f+\phi_1-\phi_2\right)\right]\\ &\quad +\frac{2\eta\left(\alpha Q_2+(1+\alpha+\eta)Q_1\right)V_0\sin\omega t}{(1+\eta)(1+2\alpha+\eta)}. \end{aligned}$$

Here, $Q_j = -2ei\partial/\partial\phi_j$, E_{J} is the Josephson energy of the Josephson junctions and f is the total magnetic flux through the loop in units of the magnetic flux quantum Φ_0. The terms on the third line of (11) represent the coupling of the flux qubit to the applied voltage $V_0\sin\omega t$. For the moment, we will consider this Hamiltonian with $V_0 = 0$.

We let $\phi_{\pm} = (\phi_1 \pm \phi_2)/2$. For $f \neq 0$, the symmetry between ϕ_1 and ϕ_2 is broken, and for f close to $1/2$, the ground and first excited states are distinguished by their behavior along the ϕ_- direction, as excitations along ϕ_+ are significantly more expensive. The typical excitation energy for $0.4 < \alpha < 0.6$ and $0.5 < f < 0.55$ is $\omega_{FQ}/2\pi = 12 - 30$GHz for $E_{\mathrm{J}}/h \sim 200$GHz and $E_{\mathrm{C}} = e^2/2C = E_{\mathrm{J}}/40$, and the nonlinearities of the spectrum are all reasonably large. In this work we will only consider flux qubits operated at the symmetry point of $f = 1/2$, in which case the ground and first excited states are both even along ϕ_+ and even or odd, respectively, along ϕ_-. From this, we can readily translate operators in the phase basis to Pauli matrices acting in the qubit basis. We will define the following compact notation for

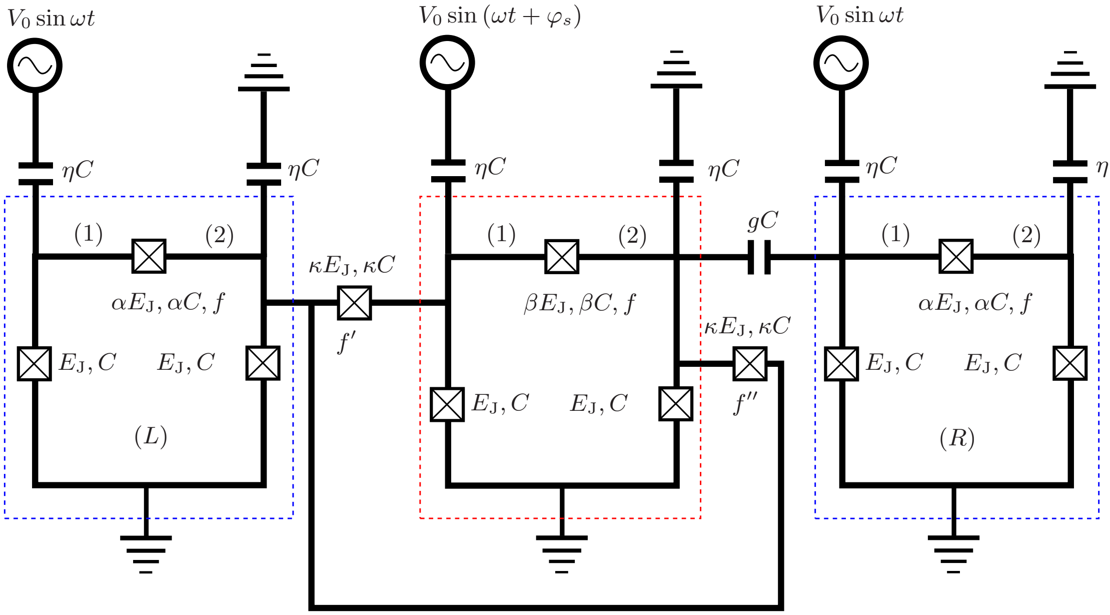

FIG. 2: (Color online) Basic circuit architecture. The regions enclosed in dashed boxes are three-junction flux qubits, which are connected to a physical ground. The blue (A, left and right) and red (B, center) qubits differ from each other by a rescaling of the area of the central Josephson junction, which is tuned so that the B qubits have higher energy excitations. A magnetic field penetrates the plane so that f flux quanta are enclosed by each ring. An oscillating voltage $V_E(t)$ is applied near resonant transitions to both qubits, mixing their ground and first excited states. Excitations in the A flux qubits can tunnel through the B qubits to each other; the oscillating voltage will make this transition matrix element complex. The qubit properties and the couplings between them are discussed in section III.

matrix elements:

$$\mathcal{M}^{ij}_{\widehat{O},s} \equiv \langle i_s | \widehat{O} | j_s \rangle \text{ e.g. } \mathcal{M}^{01}_{\mathrm{Q}_1,\mathrm{A}} = \langle 0_\mathrm{A} | \mathrm{Q}_1 | 1_\mathrm{A} \rangle . \qquad (12)$$

In this notation, we have:

$$\begin{aligned} Q_j &\rightarrow 2e\,(-1)^j\, \mathcal{M}^{01}_{\partial_{\phi_-}} \sigma^y, && (13) \\ \sin\phi_j &\rightarrow (-1)^j\, \mathcal{M}^{01}_{\sin\phi_1} \sigma^x, \\ \cos\phi_j &\rightarrow \frac{\mathcal{M}^{11}_{\cos\phi_1} + \mathcal{M}^{00}_{\cos\phi_1}}{2} \mathbf{1} + \frac{\mathcal{M}^{11}_{\cos\phi_1} - \mathcal{M}^{00}_{\cos\phi_1}}{2} \sigma^z . \end{aligned}$$

For consistency, all matrix elements $\mathcal{M}$ are calculated between the $V_0 = 0$ (non-rotating) eigenstates of the flux and transmon qubit Hamiltonians.

Let us now turn to the coupling Hamiltonian between the qubits shown in fig. 2. We label the two A qubits by L and R. The coupling of the B qubit to the right qubit is a simple capacitive coupling, and so is given by a constant times $\sigma^y_B \sigma^y_R$, which becomes a ± coupling in the rotating frame:

$$H_{BR} = \frac{8E_\mathrm{C} \mathcal{M}^{01}_{\partial_{\phi_1},B} \mathcal{M}^{10}_{\partial_{\phi_1},R}}{(1+2\alpha+\eta)(1+2\beta+\eta)} \left(\sigma^+_B \sigma^-_R + \sigma^-_B \sigma^+_R \right) . \qquad (14)$$

It is important to note that both $\sigma^x \sigma^x$ and $\sigma^y \sigma^y$ become ± couplings in the rotating frame (up to overall signs), as the components of them which lead to net creation or destruction of excitations are rapidly oscillating and should be dropped. The coupling between the left qubit and the B qubit consists of two Josephson junctions; since these junctions define closed loops through ground, they pick up flux biases f' and f'' from the external magnetic field. For simplicity, we choose the wiring geometry so that these biases are both zero mod 2π. When we write the coupling between L and B as a set of Pauli matrices, the ± terms vanish due to the sign flips in (13), but the zz term survives:

$$\begin{aligned} H_{LB} &= -2\kappa E_J \left(\mathcal{M}^{11}_{\cos\phi_1,L} - \mathcal{M}^{00}_{\cos\phi_1,L} \right) && (15) \\ &\quad \times \left(\mathcal{M}^{11}_{\cos\phi_1,B} - \mathcal{M}^{00}_{\cos\phi_1,B} \right) \sigma^z_L \sigma^z_B . \end{aligned}$$

Alternately, one could obtain a pure zz coupling by simply placing a single Josephson junction between a pair of regions, and choosing the wiring geometry so that the flux bias f' is nonzero, leading to an interaction term of the form $-\kappa E_J \cos(\phi_{L2} - \phi_{B1} + 2\pi f')$ plus a capacitive term with the same structure as (14). One could then tune f' so that the ± components of the xx and yy terms from these couplings interfere with each other, leaving only the zz part of the coupling.

We are now in a position to plug in numbers and evaluate J for this architecture. Consider flux qubits wired as in fig. 2. If we choose the realistic device parameters listed below, taking into account the single-qubit energy

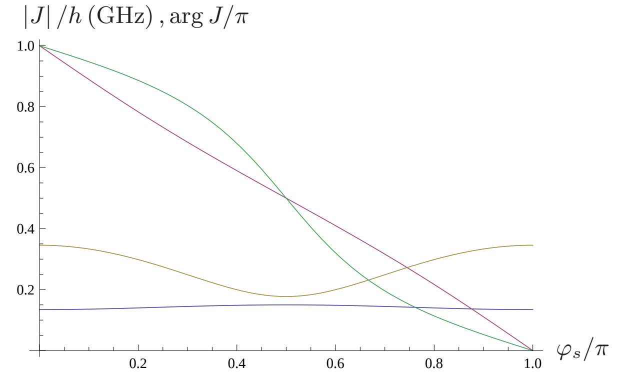

FIG. 3: (Color online) Magnitude and phase of J for the device parameters given in eq. (16) at the resonance point $\omega = \omega_A$. The blue and purple curves are $|J|$ and $\arg J/\pi$, respectively, for $V_0 = 0.5\mathrm{mV}$; the yellow and green curves are the same quantities for $V_0 = 1\mathrm{mV}$. J can be made significantly larger by increasing α and working away from the $f = 1/2$ symmetry point, but the physical device nonlinearities are smaller in that regime and the system becomes more susceptible to fluctuations in the external magnetic field.

shifts from the D^z coupling gives us:

$$\begin{aligned}
I_c &= 400\mathrm{nA},\ C = 3.25\mathrm{fF},\ \alpha = 0.5,\ f = 0.5, \qquad (16)\\
\eta &= 0.1,\ \beta = 0.45,\ \kappa = 0.2,\ g = 0.2\\
E_{\mathrm{J}}/h &= 200\mathrm{GHz} = 33E_{\mathrm{C}}/h,\ \omega_A = 2\pi\times 15.5\mathrm{GHz},\\
\omega_B &= 2\pi\times 18\mathrm{GHz},\ \frac{\Omega_{\mathrm{A}}}{\mathrm{V}_0} \simeq \frac{\Omega_{\mathrm{B}}}{\mathrm{V}_0} = 2\pi\times 4.6\frac{\mathrm{GHz}}{\mathrm{mV}},\\
D^z &= 2\pi\times 1.0\mathrm{GHz},\\
D^{\pm} &= 2\pi\times 1.4\mathrm{GHz}. \qquad (17)
\end{aligned}$$

A plot of J for $V_0 = 0.5, 1\mathrm{mV}$ is shown in figure fig. 3, calculated from (8). For small values of V_0, $|J|$ is almost completely independent of φ_s, but for larger V_0 the magnitude fluctuations become significant. $|J|$ can be further increased by up to an order of magnitude by choosing device parameters to work in the regime where $f > 1/2$, but the relative qubit nonlinearities are smaller and the system becomes more susceptible to fluctuations in the external magnetic field. We emphasize that the parameters listed above certainly do not represent the best possible choice for many-body physics, and indeed, it may ultimately turn out that other types of qubits may be superior for reaching the bosonic fractional quantum Hall regime described below. Nonetheless, they demonstrate that our system could be engineered with current technology, and achieves hopping matrix elements which are around three orders of magnitude larger than the typical flux qubit decay and dephasing rates (around a MHz).

IV. MANY-BODY STATES AND THE LOWEST LANDAU LEVEL

By considering a 2d lattice of these qubits, requiring that $|J|/(E_B - E_A) \ll 1$, and ignoring inaccessible higher excited states, we arrive at the final hopping Hamiltonian (8). Previous studies [7, 8, 11, 38–46] have shown that the square lattice version of this Hamiltonian is analogous to the 2d lowest Landau level problem of strongly interacting bosons, and realizes abelian and non-abelian fractional ground states at the appropriate fixed densities. We expect that small arrays should be sufficient to observe quantum Hall physics, since the magnetic length $l_B = 1/\sqrt{2\pi\Psi}$ (where Ψ is the gauge-invariant phase accumulated when a particle circulates around a plaquette) can be less than a lattice spacing [55]. Connections between flux qubits beyond nearest neighbors can reproduce the exact lowest Landau level of the continuum [44, 46] and lead to more robust fractional quantum Hall states, but they may not be necessary to observe the Laughlin state at $\nu = 1/2$ [7]. Here we adopt the standard definition of the filling fraction ν as the ratio of particle to flux density. A wide range of other possible quantum spin-1/2 models with 2-body interactions, both with complex phases and without, could be studied in this device architecture; we find quantum Hall systems to be the most intriguing, due to the existence of abelian anyons at $\nu = 1/2$ and the existence (with tuning) of non-abelian anyons at $\nu = 1$ and $3/2$ [5, 46], along with other exotic states at different filling fractions. The boson density could be controlled by using a second external field at frequency ω' near $2\Omega_A$ to populate the lattice; the ω' dependence of the system's response to this field could be used to measure the gaps of the many-body states.

The incoherent particle gain and loss rates in our array from single qubit decay and dephasing effects should not be a significant obstacle to studying strongly correlated many-body states. Using values from the previous section and from the superconducting qubit literature [21, 47], a typical hopping parameter would be $J/\hbar = 1\mathrm{GHz}$. It is important to note here that the particles in our case are rotating frame antisymmetric superpositions of the ground and first excited states of the physical qubits, so their decay would be from one type of superposition to the other. This rate would be roughly given by the dephasing rate of the qubits, which for flux qubits is of order 1MHz. With a Landau band spacing of $\omega_{\mathrm{LLL}} \simeq 3J$ in a square lattice at $\Psi = 1/4$ quanta per plaquette, the relative correction to the Landau bandwidth from this process decay would be thus be insignificant. We expect that this loss rate by itself will not prevent quantum Hall states from forming in our array [25]. Likewise, a small number of "dead" sites (where a qubit is defective and cannot be excited) should also be relatively harmless– the many-body wavefunction can eliminate these defects simply by nucleating a quasihole at each site. So long as the density of flux quanta is large compared to the defect density, these defects will simply make small shifts in the gap energy and particle density of the gapped states, but will not have any other qualitative effects on the system.

More worrisome is the issue of time-independent random variations in the qubit properties at every site, which could disrupt the formation of topological states if these variations became large enough. To quantify this issue, we numerically simulated the broadening of the lowest Landau level in our model as a function of three static (quenched) noise sources: random fluctuations in the on-site potential (shifts in the rotating frame excitation energy of a given A qubit), random fluctuations in the magnitude of J, and random fluctuations in the phase of J between neighboring sites. In a real system, these noise sources would be correlated, but as the details of those correlations would depend in part on the physical implementation of the qubits, we have assumed that each type of quenched disorder is applied randomly to every site with no dependence on the other types or on the disorder at nearby sites. To determine the broadening from each noise source, we numerically diagonalized the single-particle hopping matrix on 8×8 and 12×12 lattices with periodic boundary conditions, given by the Hamiltonian:

$$\begin{aligned} H_{LLL} &= \sum_{ij} \left(F_{ij}\right) J_{ij} \left(e^{i(\phi_{ij}+\pi\delta\phi_{ij})} + H.C.\right) \\ &+ \sum_{i} J_{NN}\delta U_i n_i. \end{aligned} \tag{18}$$

Here, the hopping matrix elements are restricted to nearest and next nearest neighbors with relative magnitudes chosen as in [44], δU_i and $\delta\phi_{ij}$ are dimensionless parameters which are Gaussian distributed about 0, J_{NN} is the average nearest neighbor hopping energy, and F_{ij} is a dimensionless parameter which is Gaussian distributed about 1. We diagonalized (18) for 25 random distributions of noise for each data point, and from the spectrum we extracted the lowest Landau level broadening Δ, which is the ratio of the energy splitting between the lowest and highest LLL states to the splitting between the highest LLL state and the bottom of the first excited band. We then fit $\Delta\left(\sigma_{U/J/\Psi}\right)$ as a function of the standard deviation of each noise source with the other two sources set to zero; this relationship was linear in each case for small fluctuations. The results of our simulations are shown in table I; note that Δ_0 is nonzero even without defects, as a consequence of truncating the Hamiltonian in [44] to nearest and next nearest neighbor hopping.

It is important to note that this calculation only captures distortions to the single particle spectrum and that the many-body response to noise of this type is a subtle problem beyond the scope of this work. However, we qualitatively expect that the topological states should be disrupted when the normalized Landau level splitting Δ approaches the dimensionless quasiparticle excitation gap Δ_{qp}/J_{NN}. In numerical studies of this system in the clean limit with hard-core 2-body repulsion (largely unpublished), Δ_{qp}/J_{NN} typically ranged between 0.2 and 1 for correlated states at different flux and particle densities, and tended to be larger at smaller filling fractions. This suggests that many-body quantum Hall states should exist in our system when noise is sufficiently well-controlled.

Flux Density	Δ_0	C_U	C_J	C_Ψ
1/4	0.015	0.41	1.42	1.75
1/3	0.018	0.72	1.21	2.36
3/8	0.08	0.35	0.99	1.94

TABLE I: Robustness of the lowest Landau level to external noise sources. For the random noise simulations described in the text, we fit the normalized splitting Δ of the lowest Landau level to the function $\Delta = \Delta_0 + C_U\sigma_U + C_J\sigma_J + C_\Psi\sigma_\Psi$, where the σ's are the standard deviation of each noise source (local potential, hopping magnitude, and hopping phase) which is applied randomly to every site (σ_U) and link between sites (σ_J and σ_Ψ). As seen in the Hamiltonian (18), the potential fluctuations are in units of J_{NN} and the phase fluctuations are in units of π. Above the flux density $\Psi = 1/3$, truncation to nearest and next nearest neighbor hopping introduces significant broadening even in the clean system, so flux densities of 1/3 or less should be the focus of experiments on our design.

V. A SIMPLE EXPERIMENT TO DEMONSTRATE THE GAUGE FIELD

While the ultimate purpose of this proposal is to study exotic many-body states in an array of hundreds or thousands of flux qubits, the existence of a nontrivial gauge field can be demonstrated by studying an arrangement of four flux qubits, connected in a loop. Consider a square loop of four flux qubits labeled (1-4), where qubit 1 sits at the top left corner and qubit 4 at the bottom right, as shown in Fig. 4. For this choice, any hop through a D^z coupling will accumulate a phase ψ, giving a total of $\Psi = 2\psi$ for a complete circuit of the loop. Conversely, if the phases of the voltages applied to the B qubits are shifted by π from one FQ-FQ pair to the next, the magnitude of the hopping matrix element will be unchanged but there will be no complex phase accumulation. In this case, the B qubits have identical rotating frame energies to the A qubits, and differ from them through the relative phases φ_{si} of the applied voltages. We will assume for simplicity that the magnitudes of the hopping matrix elements from the D^z and $D^\pm$ couplings are both equal to J.

To demonstrate that the alternating voltages generate a nonzero effective flux through the four-qubit loop, we first initialize the array by letting all four qubits relax to their ground states. At time $t = 0$, we apply a microwave pulse to qubit 1 to excite it into the fluxon state $|1\rangle$, and then at time t we measure the state of qubit 4. The probability of qubit 4 being occupied by the fluxon is given by

$$\begin{aligned} P_4(t) &= \left|\langle 0_1 0_2 0_3 1_4|\, e^{iHt/\hbar}\, |1_1 0_2 0_3 0_4\rangle\right|^2 \\ &= \frac{1}{4}\left(\cos\left(\frac{2tJ}{\hbar}\cos\frac{\Psi}{4}\right) - \cos\left(\frac{2tJ}{\hbar}\sin\frac{\Psi}{4}\right)\right)^2. \end{aligned} \tag{19}$$

This interference pattern is particularly striking when Ψ is nearly equal to π. If we let $\Psi = \pi + \epsilon$, the probability distribution becomes

$$P_4\left(t\right) = \left(\sin\frac{\sqrt{2}Jt}{\hbar}\right)^2 \left(\sin\frac{Jt\epsilon}{2\sqrt{2}\hbar}\right)^2 . \tag{20}$$

In the limit of $\epsilon \to 0$, the probability of qubit 4 being occupied becomes zero at all times, due to the perfect interference of the two paths. This is a dramatic effect, and while field fluctuations and fabrication defects would prevent perfect interference in a real device, the strong slowing of the occupation periodicity of qubit 4 as Ψ approaches π would be readily observable. Such interference is only possible if there is a gauge-invariant phase difference between the two paths, and would therefore demonstrate that nontrivial effective gauge fields are realized in our architecture.

VI. CONCLUSION

We have demonstrated a method for realizing a quantum Hall state of bosons using asymmetric qubit pairs, driven by applied oscillating electric fields. We also demonstrated that our model could be implemented in a lattice of flux qubits. With appropriate protocols for stabilizing the average particle density and measuring the conductivity, we expect that conductivity quantization could be observed on small arrays, though we note that the details of how to measure the conductivity are beyond the scope of this article. The statistics of anyonic collective modes could be determined through similar methods [48–51].

Further, the dynamical tunability of our model could be exploited to realize exotic combinations of states that would be difficult or impossible to study in cold atom or solid state systems. One could locally adjust the applied voltage $V_0 \sin\left(\omega t + \varphi_s\right)$ and flux bias f to change the gauge field density and effective chemical potential in a given region, creating islands of arbitrary shape which could be at a different filling fraction than the surrounding lattice and thus have different anyonic modes. Alternately, by reversing the signs of all the phase shifts φ_s in a region, one can crate a sharp boundary between regions with effective gauge fields of equal magnitude but opposite sign. In both cases, we expect physics along the boundaries to be rich.

Finally, by locally tuning V_0, φ_s and f to manipulate vortices in the qubit lattice, arrays of ordinary qubits could be used to construct a topological non-abelian anyon qubit [4, 5, 52], trading information density for topological protection against decoherence. In that sense our proposal is similar to the surface code and cluster state [53, 54] ideas developed in recent years, and provides a new potential mechanism for reducing decoherence in superconducting quantum information devices.

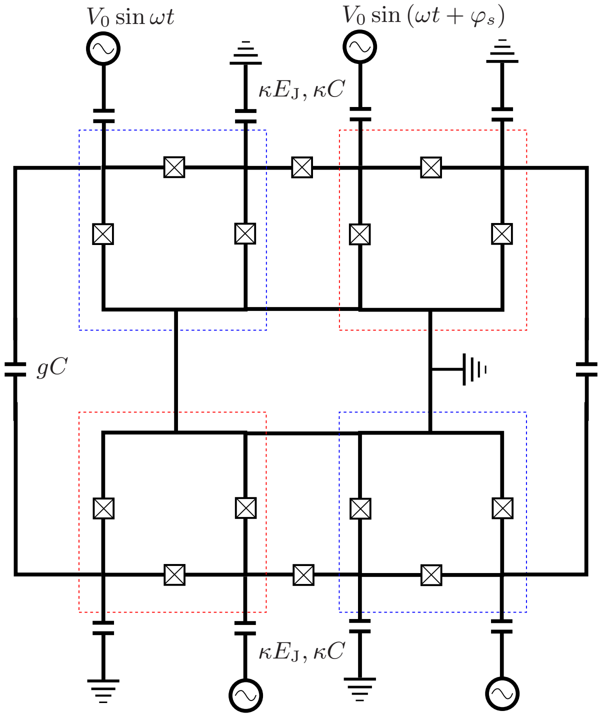
$V_0 \sin \omega t$
$V_0 \sin\left(\omega t + \varphi_s\right)$
$\kappa E_{\mathrm{J}}, \kappa C$
gC
gC
$\kappa E_{\mathrm{J}}, \kappa C$

FIG. 4: (Color online) Configuration to demonstrate the artificial gauge field, as outlined in section V. As described in section V, appropriately tuning the phase offsets φ_{si} will produce a gauge-invariant phase difference in the two paths that the mobile fluxon excitation could take from qubit 1 to qubit 4. The resulting interference of these two paths can be detected in the time-dependent probability $P_4\left(t\right)$ of qubit 4 being in its excited state.

VII. ACKNOWLEDGMENTS

We would like to thank John Chalker, Greg Fuchs, Chris Henley, Matteo Mariantoni, John Martinis and Dan Ralph for useful discussions related to this project. We are indebted to Paul Ginsparg for his critical comments and advice, and to Steve Simon for his assistance in the final preparation of this manuscript. Most of all, we would like to thank Erich Mueller for his guidance at many stages of this project. This material is based on work supported in part by the National Science Foundation Graduate Program, EPSRC Grant No. EP/I032487/1, and Oxford University.

[1] R. B. Laughlin, Phys. Rev. Lett. **50**, 1395 (1983).
[2] R. E. Prange and S. M. Girvin, *The Quantum Hall Effect* (Springer, 1986).
[3] D. Yoshoika, *The Quantum Hall Effect* (Springer-Verlag,

1998).

[4] A. Kitaev, Ann. Phys. **303**, 2 (2003).

[5] C. Nayak, S. H. Simon, A. Stern, M. Freedman, and S. D. Sarma, Rev. Mod. Phys. **80** 1083 (2008).

[6] N. R. Cooper, N. K. Wilkin, and J. M. F. Gunn, Phys. Rev. Lett. **87**, 120405 (2002).

[7] M. Hafezi, A. S. Sorensen, E. Demler, and M. D. Lukin, Phys. Rev. A **76**, 023613 (2007).

[8] A. S. Sorensen, E. Demler, and M. D. Lukin, Phys. Rev. Lett. **94**, 086803 (2005).

[9] N. R. Cooper, Advances in Physics **57**, 539 (2009).

[10] G. Moller and N. R. Cooper, Phys. Rev. Lett. **103**, 105303 (2009).

[11] L. Hormozi, G. Moller, and S. H. Simon, Phys. Rev. Lett. **108**, 256809 (2012).

[12] B. J.-D. *et al*, Phys. Rev. A **84**, 053605 (2011).

[13] B. Juliá-Díaz, T. Graβ, N. Barberán, and M. Lewenstein, New J. Phys. **14**, 055003 (2012).

[14] J. Dalibard, F. Gerbier, G. J. unas, and P. Öhberg, Rev. Mod. Phys. **83**, 1523 (2011).

[15] I. Bloch, J. Dalibard, and W. Zwerger, Rev. Mod. Phys. **80**, 885 (2008).

[16] M. Y. Choi, Phys. Rev. B **50**, 10088 (1994).

[17] A. Stern, Phys. Rev. B **50**, 10092 (1994).

[18] R. Fazio and H. van der Zant, Phys. Rep. **355**, 235 (2001).

[19] H. S. J. van der Zant, W. J. Elion, L. J. Geerligs, and J. E. Mooij, Phys. Rev. B **54**, 10081 (1996).

[20] Y. Makhlin, G. Schoen, and A. Shnirman, Rev. Mod. Phys. **73**, 357 (2001).

[21] J. Clarke and F. K. Wilhelm, Nature **453**, 1031 (2008).

[22] A. Nunnenkamp, J. Koch, and S. M. Girvin, New J. Phys. **13**, 095008 (2011).

[23] M. Hafezi, E. Demler, M. Lukin, and J. Taylor, Nature Physics 7, 907–912 (2011) (2011).

[24] R. O. Umucalilar and I. Carusotto, Phys. Rev. A **84**, 043804 (2011).

[25] M. Hafezi, M. D. Lukin, and J. M. Taylor, arXiv:1301.1344v1 (2013).

[26] J. E. Mooij, T. P. Orlando, L. Levitov, L. Tian, C. H. van der Wal, and S. Lloyd, Science **285**, 1036 (2001).

[27] T. P. Orlando, J. E. Mooij, L. Tian, C. H. van der Wal, L. S. Levitov, S. Lloyd, and J. J. Mazo, Phys. Rev. B **60**, 15398 (1999).

[28] I. Chiorescu, Y. Nakamura, C. Harmans, and J. Mooij, Science **299**, 1869 (2003).

[29] A. O. Lyakhov and C. Bruder, New. J. Phys. **7**, 181 (2005).

[30] J. B. Majer, F. G. Paauw, A. C. J. ter Haar, C. J. P. M. Harmans, and J. Mooij, Phys. Rev. Lett 94, 090501 (2005).

[31] M. G. *et al*, Phys. Rev. B **72**, 020503 (2005).

[32] S. Matsuo, K. Furuta, T. Fujii, K. Nagai, and N. Hatakenaka, Appl. Phys. Lett. **91**, 093103 (2007).

[33] K. Kakuyanagi, T. Meno, S. Saito, H. Nakano, K. Semba, H. Takayanagi, F. Deppe, and A. Shnirman, Phys. Rev. Lett. **98**, 047004 (2007).

[34] J. Bourassa, J. M. Gambetta, A. A. A. Jr, O. Astafiev, Y. Nakamura, and A. Blais, Phys. Rev. A 80, 032109 (2009).

[35] L. Jiang, C. L. Kane, and J. Preskill, Phys. Rev. Lett. 106, 130504 (2011).

[36] J. Koch, A. A. Houck, K. L. Hur, and S. M. Girvin, Phys. Rev. A **82**, 043811 (2010).

[37] A. Nunnenkamp, J. Koch, and S. M. Girvin, New J. Phys. **13**, 09500 (2011).

[38] D. Hofstadter, Phys. Rev. B **14**, 2239 (1976).

[39] M. Kohmoto, Phys. Rev. B **39**, 11943 (1989).

[40] F. F. Assaad and S. Biskamp, Phys. Rev. B **51**, 1605 (1995).

[41] R. N. Palmer, A. Klein, and D. Jaksch, Phys. Rev. A **78**, 013609 (2008); R. N. Palmer and D. Jaksch, Phys. Rev. Lett. **96**, 180407 (2006) (????).

[42] C. Zhang, V. W. Scarola, S. Tewari, and S. D. Sarma, PNAS **104**, 18415 (2007).

[43] R. O. Umucalilar, H. Zhai, and M. Oktel, Phys. Rev. Lett. **100**, 070402 (2008).

[44] E. Kapit and E. Mueller, Phys. Rev. Lett. **105**, 215303 (2010).

[45] R. O. Umucalilar and E. J. Mueller, Phys. Rev. A **81**, 053628 (2010).

[46] E. Kapit, P. Ginsparg, and E. Mueller, Phys. Rev. Lett. **108**, 066802 (2012).

[47] F. Yoshihara, K. Harrabi, A. O. Niskanen, Y. Nakamura, and J. S. Tsai, Phys. Rev. Lett. 97, 167001 (2006).

[48] S. D. Sarma, M. Freedman, and C. Nayak, Phys. Rev. Lett. **94**, 166802 (2005).

[49] P. Bonderson, A. Kitaev, and K. Shtengel, Phys. Rev. Lett. **96**, 016803 (2006).

[50] R. L. Willett, L. N. Pfeiffer, and K. W. West, Phys. Rev. B **82**, 205301 (2010).

[51] S. A. *et al*, arXiv:1112.3400 (2011).

[52] L. Hormozi, G. Zikos, N. E. Bonesteel, and S. H. Simon, Phys. Rev. B **75**, 165310 (2007).

[53] X.-C. Y. *et al*, Nature **482**, 489 (2012).

[54] A. G. Fowler, M. Mariantoni, J. M. Martinis, and A. N. Cleland, arXiv:1208.0928 (2012).

[55] We calculate the magnetic length by analogy to the mapping to the lowest Landau level in [44]; the coefficient of the Gaussian in the Landau level wavefunctions sets l_B.